Fluoride 2020 Jan 4. www.fluorideresearch.online/epub/files/071.pdf [Epub ahead of print]

SYNTHESIS OF MAGNETIC COBALT FERRITE NANOPARTICLES FOR THE REMOVAL OF EXCESS FLUORIDE IONS FROM AQUEOUS SOLUTIONS

Fatemehsadat Masoudi,[a] Ali Naghizadeh,[b],* Mohammad Kamranifar,[a] Amir Hossein Mahvi[c]

Birjand and Tehran, Iran

ABSTRACT: The aim of this study was to evaluate, using batch methodology, the effect of various parameters such as pH, adsorbent dose, contact time, magnetic fluoride concentration, and temperature on fluoride adsorption using cobalt ferrite nanoparticles ($CoFe_2O_4$NPs). The adsorption parameters were determined by the Langmuir, Freundlich, Temkin, and Dubinin-Radushkevich isotherm models and pseudo-first-order kinetics and pseudo-second-order kinetics. Finally, the thermodynamic parameters (ΔH, ΔS, and ΔG) of fluoride adsorption on magnetic cobalt ferrite nanoparticles were considered. The results showed that in optimum conditions for fluoride adsorption by magnetic cobalt ferrite nanoparticles, pH=3, adsorbent dose=0.2 g/L, fluoride concentration=10 mg/L, contact time=10 min, the maximum absorption capacity is 8.75 mg/g. The adsorption process follows the Langmuir isotherm and pseudo-second-order kinetics. In the study of the thermodynamic results of the adsorption process, positive values of ΔS and ΔH and a negative value of ΔG were obtained

Key words: Adsorption; Cobalt ferrite; Fluoride; Magnetic nanoparticles.

INTRODUCTION

The quality of drinking water may have a significant impact on the health of a community and therefore the chemical nature of surface water and ground water is a criterion to be considered in the selection of the drinking water sources in communities.[1] Fluorine, one of the elements of the earth's crust, the most electronegative element, and located in the group of halogens in the periodic table. has a strong tendency to combine with cations, and therefore it is not found in a free state in nature. Fluorine forms several mineral compounds, including cryolite, fluorapatite, and fluorspar. Fluoride, the ion of fluorine, is mainly released into groundwater through the dissolution of fluoride-containing rocks.[2-5] The discharge of agricultural and industrial sewage, such from the production of aluminum, steel, glass, etc., also causes large amounts of fluoride to enter ground water.[6] Fluoride contamination in water is a major problem across the globe and, although upper limits for fluoride in drinking water of approximately 0.5 to 1.5 mg/L have been recommended by some, including the World Health Organization,[7-9] a recent review estimated the benchmark dose level (BMDL, the lower one-sided 95% confidence limit of the benchmark dose [BMD], for pregnant women to prevent developmental neurotoxicity in the foetus is about 0.2 mg/L or lower.[10] Available statistics show that the fluoride ion level in drinking water may reach 20 mg/L in areas of northern Africa.[6] Also, in some cities of Iran, the fluoride content is higher than 1.5 mg/L.[11] Fluoride in drinking water can cause dental, skeletal, and non-skeletal fluorosis.

---

[a]Student Research Committee, Faculty of Health, Birjand University of Medical Sciences (BUMS), Birjand, I.R. Iran; [b]Medical Toxicology and Drug Abuse Research Center (MTDRC), Birjand University of Medical Sciences (BUMS), Birjand, I.R. Iran; [c]Center for Solid Waste Research, Institute for Environmental Research, Tehran University of Medical Sciences, Tehran, Iran. *For correspondence: Ali Naghizadeh, Medical Toxicology and Drug Abuse Research Center (MTDRC), Birjand University of Medical Sciences (BUMS), Birjand, I.R. Iran; Tel: +985632381665, Fax: +985632395346, E-mail: al.naghizadeh@yahoo.com

Fluorosis weakens the structure of the teeth and skeletal system and can slow down growth. High concentrations of fluoride can lead to health hazards such as headache, depression, digestive disorders, nausea, impaired cognitive functioning, decreased immunity, and abortion.[2,12,13] Many research publications in Iran have reported on fluoride in air, food, and water.[14-19]

Given the adverse effects of fluoride ion in drinking water, especially water from groundwater resources, the main source of drinking water in most societies, it is necessary to consider the removal of excess fluoride from water. Many methods have been used to remove excess fluoride from the water including adsorption, chemical precipitation, and electro dialysis.[20-23] The absorption process is commonly used as an affordable, nature-friendly method to remove pollutants from water sources.[24] The adsorption process is usually carried out on activated carbon. However, activated carbon is an expensive adsorbent and this has restricted its use.[25] Other adsorbents used to remove fluoride include montmorillonite,[26] bone charcoal,[27] and zeolite.[28] So far, the efficiency of magnetic cobalt ferrite nanoparticles ($CoFe_2O_4$NPs) has not been investigated in the removal of fluoride ion from water. Magnetic $CoFe_2O_4$-TiO_2NPs containing titanium dioxide-based spinel ferrite can be retrieved and reused.[29] The advantages of these nanoparticles include resistance to chemicals, mechanical blows, and heat.[30,31] The aims of this study were to investigate, using a batch flow process, the efficiency of synthesized magnetic ferrite cobalt nanoparticles in removing excess fluoride from aqueous solutions and to examine the effects of pH, adsorbent dose, reaction time, initial fluoride concentration, and temperature on the adsorption process.

MATERIALS AND METHODS

The materials needed in this study were cobalt nitrate powder, iron nitrate powder, soda, sodium fluoride, and SPADNS solution purchased from Merck Company. Deionized water was used in all experiments. In order to determine the concentration of residual fluoride a spectrophotometer DR6000 (Hach) was used, the samples were mixed with a shaker (multishaker, Model NB-101MT, Korea), a pH meter was used to determine pH (pH meter HQ411d, Hach), and an incubator shaker (combishaker, Model NB-101MT) was used for temperature stability.

Firstly, a solution containing 0.021 mole of cobalt nitrate powder, 0.002 mole of iron nitrate powder, and 100 mole of deionized water was prepared. Then 20 mole of soda were added slowly. The solution is placed at 80ºC for 2 hours. After that, the magnetic nanoparticles were separated from the solution using a magnet and washed with deionized water. Finally, put the powder was placed in an oven to dry.[32] The properties of the synthesized nanoparticles were investigated by a scanning electron microscope (SEM), a transmission electron microscope (TEM), Fourier transform infrared spectroscopy (FTIR), X-ray diffraction (XRD), and a vibrating-sample magnetometer (VSM). In this study, the experiments were carried out with the variables of pH (3, 5, 7, 9, and 11), concentration of synthesized cobalt ferrite (0.2, 0.4, 0.6, and 0.8 g/L), initial concentration of contaminant (1, 2, 5, and 10 mg/L), contact time (5, 10, 20, 40, 60, and 90 min), and temperature (15, 25, 35, and 45ºC). Fluoride stock solution was prepared by dissolving 0.221 mg of sodium fluoride salt in 1 L of deionized water and fluoride solutions were obtained from dilution of the stock solution. 1 and 0.1 N HCL & NaOH were used to set pH. Solutions were placed on a 250 round shaker and after a specific time, the adsorbent was separated from filter by filter paper and the remaining pollutants were measured by the spectrophotometer. The investigation of the optimum adsorption conditions was determined by the influence of variables including pH, adsorbent dose, contact time, initial fluoride concentration, and temperature. At first, the effect of pH solution on fluoride adsorption by cobalt ferrite was determined in the range of 3 to 11 and the optimal pH was determined. Then, at the optimal pH, the effect of adsorbent dose on the adsorption process was investigated. In next step, the effect of the contact time and the initial fluoride concentration was investigated using pH and adsorbent dose and finally, by adjusting the other variables, the effect of temperature on the adsorption process was investigated. The following formula was used to calculate the adsorption capacity of magnetic $CoFe_2O_4NPs$ in the removal of fluoride (mg/g).

$$q_e = \left(\frac{C_0 - C_e}{M}\right) \times V \qquad (1)$$

Where, C_o is the initial fluoride concentration in the solution (mg/L), C_e is the residual fluoride concentration at the equilibrium moment (mg/L), V is the sample volume (L), and M is the mass of $CoFe_2O_4NPs$ in grams.[33]

ISOTHERM MODELS:

In this study the Langmuir, Freundlich, Brunauer-Emmett-Teller theory (BET), Temkin, and Dubinin-Radushkevich adsorption isotherm models were used for mathematical modeling.

Langmuir model:

$$\frac{C_e}{q_e} = \frac{1}{q_m K_L} + \frac{C_e}{q_m} \qquad (2)$$

Where, q_e is the amount of adsorbed fluoride per unit mass of adsorbent (mg/g), C_e is the fluoride concentration in the solution at the equilibrium moment (mg/L), q_m is the maximum adsorption capacity (mg/g), and K is the Langmuir constant.[26] The dimensionless parameter R_L (separation factor) is a property of the Langmuir equation which is calculated using equation 3. Using this parameter, the type of adsorption process can be determined.

$$R_L = \frac{1}{(1+bC_0)} \qquad (3)$$

Where, $R_L>1$ is undesirable adsorption, $R_L=1$ is linear adsorption, $R_L=0$ is irreversible adsorption, and $0<R_L<1$ is desirable adsorption.[34]

Freundlich model:

$$\log q_e = \log K_F + \frac{1}{n} \log C_e \qquad (4)$$

Where, q_e is the amount of adsorbed fluoride in (mg/g), C_e is the concentration of adsorbed fluoride in solution at equilibrium moment (mg/l), and 1/n and k_f are Freundlich constants. Therefore, the graph $\log q_e$ against $\log C_e$ is a straight line whose gradient is 1/n and its y-intercept is $\log k_f$.[35]

BET isotherm equation:

$$\frac{C_e}{Q_e(C_s - C_e)} = \frac{1}{K_b Q_{max}} + \frac{K_b - 1}{K_b Q_{max}} \times \frac{C_e}{C_s} \qquad (5)$$

Where, C_s is the saturation concentration of solute in mg/L, K_b is a constant obtained through the equation and represents the energy between the adsorbate and the adsorbent surface and it has a direct relationship with adsorption energy, and Q_{max} is the adsorbate value per unit mass of adsorbent (g) to form a single molecular layer on the adsorbent (mg/g).[35]

Temkin linear isotherm:

$$q_e = B \ln A_T + B \ln C_e \qquad (6)$$

In this equation B= R_T/b_T. R is known as the gas constant (R=8.314 $J.K^{-1}.mol^{-1}$) and T is the absolute temperature in Kelvin. Using the isotherm A and B curves, the gradient and y-intercept of the curve were determined, respectively. In this equation, A_T (L/mg) is a bond constant related to the maximum bond energy, and b_T(J/mol) is the Temkin isothermal constant that is proportional to the adsorption heat.[36]

Dubinin-Radushkevich isotherm:

$$\ln q_e = \ln q_m - \beta\varepsilon^2 \qquad (7)$$

Where, q_e is the amount of fluoride adsorbed on the magnetic $CoFe_2O_4$NPs (mg/g) in the equilibrium state and q_m is the adsorption capacity of adsorbent on per unit mass. The parameter β is the Dubinin-Rudeshkuvich adsorption constant and is a potential which is described by function 8:

$$\varepsilon = RT \ln\left(1 + \frac{1}{C_e}\right) \qquad (8)$$

Where, R is the gas constant, T is the Kelvin temperature, and C_e is the equilibrium concentration of soluble matter in solution. Then, the graph of $\ln q_e$ against ε will be a line from which the β value is obtained from the gradient of the line and according to equation 9 information about the adsorption energy, E, (kj/mol) can be obtained.[37]

$$E = \frac{1}{\sqrt{-2B}} \qquad (9)$$

KINETICS OF THE ABSORPTION PROCESS:

In this study, the pseudo-first-order and the pseudo-second-order kinetic equations were used to analyze the test data. The linear equations of the kinetics are as follows:

Pseudo-first-order:

$$\ln(q_e - q_t) = \ln(q_e - K_1) \qquad (10)$$

Pseudo-second-order:

$$\frac{t}{q_t} = \frac{1}{K_2 q_0^2} + \frac{1}{q_0} t \qquad (11)$$

Where, qe (mg/g) is the adsorbed fluoride on the adsorbent surface at time t (min), K_1 is the pseudo-first-order constant (min^{-1}), and K_2 is the pseudo-second-order constant (g/mg/min).[33]

THERMODYNAMICS OF THE ADSORPTION PROCESS:

Equation 12 was used to study the thermodynamics of the adsorption process:

$$\Delta G = -RT(\ln K_C) \qquad (12)$$

Where, ΔGº is the Gibbs free energy (kJ/mol), R is the gas constant (8.134 J/mol/K) and T is the absolute temperature (K). The parameters of the standard enthalpy ΔHº and the standard entropy ΔSº in the adsorption process are calculated by equations 13 and 14.

$$\ln K_c = \frac{\Delta S^\circ}{R} - \frac{\Delta H^\circ}{RT} \qquad (13)$$

$$K_c = \frac{q_e}{C_e} \qquad (14)$$

Where, K_c (L/g) is the ratio of the amount of fluoride adsorbed on the adsorbent (mg/g) to the residual amount of fluoride in solution (mg/L). To determine the thermodynamic parameters of the process, the curve $\ln k_c$ against 1/T was used. The slope of the resulting line represents the ΔH value (kJ/mol) and the y-intercept indicates the ΔSº (J/mol K).[32]

RESULTS

Specification of the synthesized absorbent: Figure 1 shows the scanning electron microscopy (SEM) images of magnetic $CoFe_2O_4$NPs. The analysis of the morphology of nanoparticles shows that the diameter of the nanoparticles is less than 100 nm.

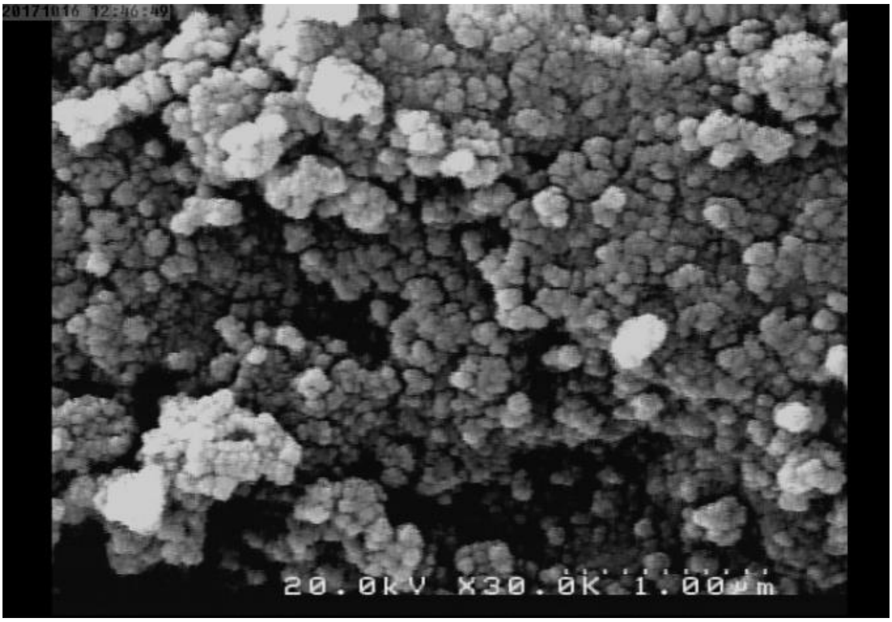

Figure 1. Scanning electron microscopy (SEM) images of magnetic $CoFe_2O_4$NPs.

The transmission electron microscopy (TEM) image of magnetic $CoFe_2O_4$NPs is shown in Figure. 2. Analysis of the size of the nanoparticles by TEM analysis showed that the diameter of the nanoparticles was less than 100 nm.

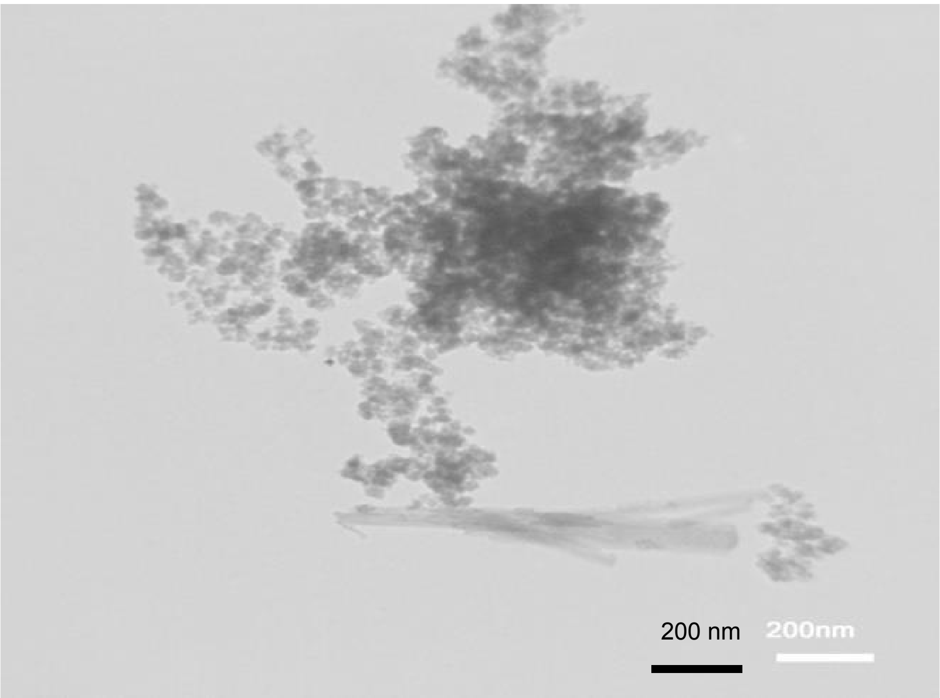

Figure 2. Transmission electron microscopy (TEM) images of magnetic $CoFe_2O_4$NPs.

FTIR analysis: In Figure 3, the results of the FTIR spectrum scan of the magnetic $CoFe_2O_4$NPs are shown. The range of the spectrum was 400–4000 cm^{-1}. The specified peaks in this spectrum are: 3406 cm^{-1} (OH and -NH2), 1625 cm^{-1} (C=C group), 1360 cm^{-1} (C-H group), 898 and 963 cm^{-1} (OH out plane vibration), and 410 and 600 cm^{-1} (presence of ferrite nanoparticles).[38]

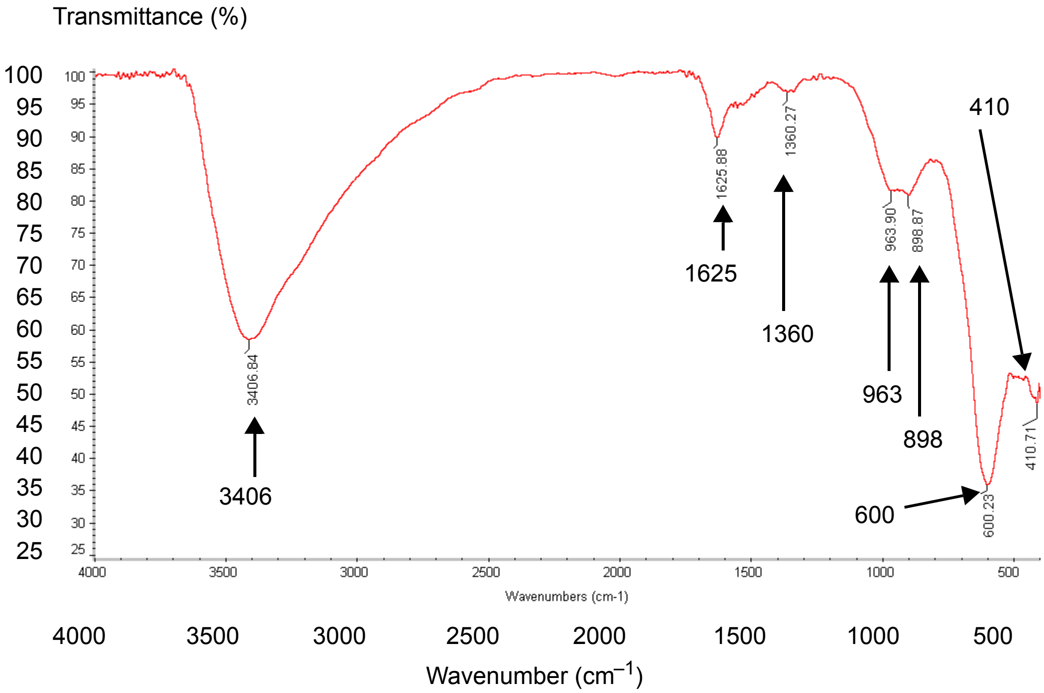

Figure 3. Fourier transmission infrared spectroscopy (FTIR) spectrum of magnetic $CoFe_2O_4$NPs.

XRD analysis: Figure 4 shows the images of the X-ray diffraction (XRD) analysis of the magnetic $CoFe_2O_4$NPs. The location and intensity of the peaks represent the crystalline structure and the cubic spline of the formed nanoparticles which is very close to the (literature) values with JCPDS NO.01-1121. In addition, the average grain size of the synthesized nanoparticles, calculated by the Scherer formula, was 8 nanometers.[32]

VSM analysis: The ferromagnetic hysteresis loop of the magnetic $CoFe_2O_4$NPs is shown in Figure 5. The saturation magnetization value for the cobalt ferrite magnetic nanoparticles was 42 emu/g.

Determination of pHzpc: Deionized water solutions with a pH range of 2 to 12 were prepared to determine the pH point of zero charge (pHzpc) using HCl and NaOH. Then, 25 mg of magnetic $CoFe_2O_4$NPs were added to 50 mL of the solution. After 24 hours, the pH of the solutions measured by the pH meter. Figure 6 shows that pHzpc for magnetic $CoFe_2O_4$NPs was about 7.3.

Effect pH on adsorption process: In Figure 7, the effect of the pH in the range of 3–11 on the fluoride adsorption by the magnetic $CoFe_2O_4$NPs is shown. In the present study, solutions containing 1 mg/L fluoride were prepared. After adjusting the pH to 3, 5, 7, 9, and 11, 0.5 g of adsorbent dose was added to each of the solutions. After 60 minutes, the concentration of residual fluoride in the solution was measured by a spectrophotometer. The maximum fluoride adsorption occurred at pH=3. This pH was therefore selected as the optimum pH for the adsorption process. The fluoride adsorption capacity by these nano particles at this pH was 1.28 mg/g.

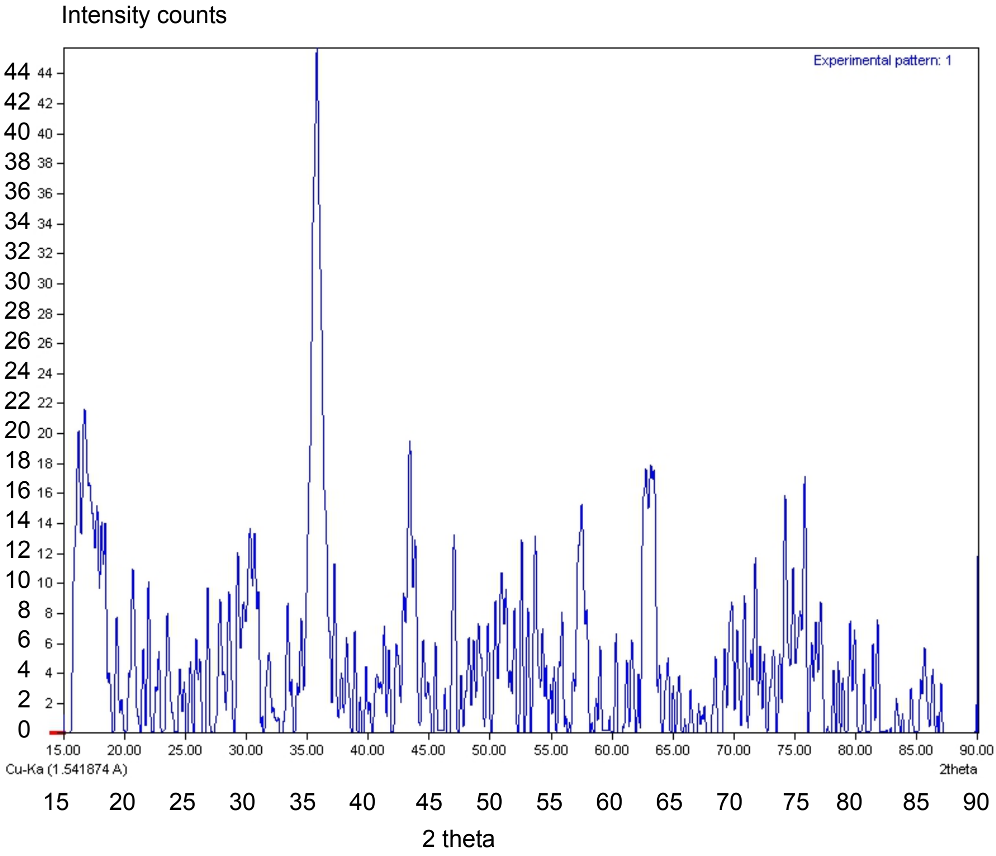

Figure 4. X-ray diffraction (XRD) analysis of magnetic CoFe2O4NPs.

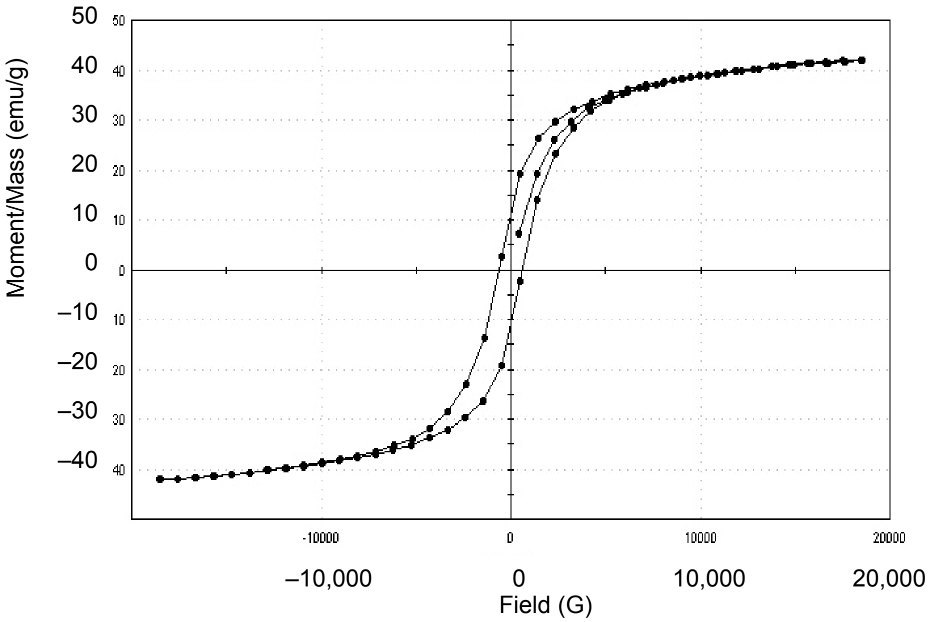

Figure 5. Vibrating sample magnetometer (VSM) analysis of magnetic CoFe2O4NPs.

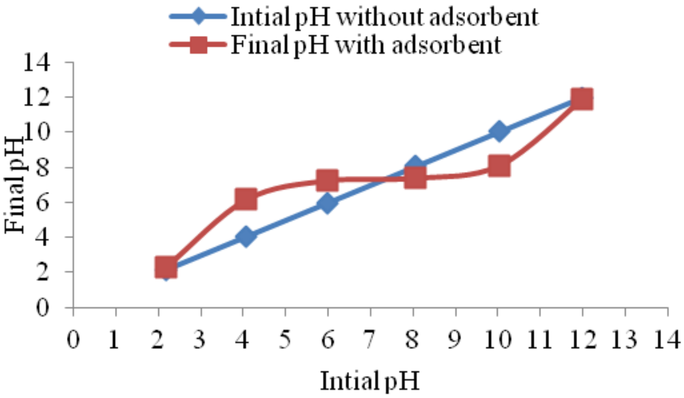

Figure 6. Determination of the pH point of zero charge (pHzpc) pH for magnetic $CoFe_2O_4$NPs.

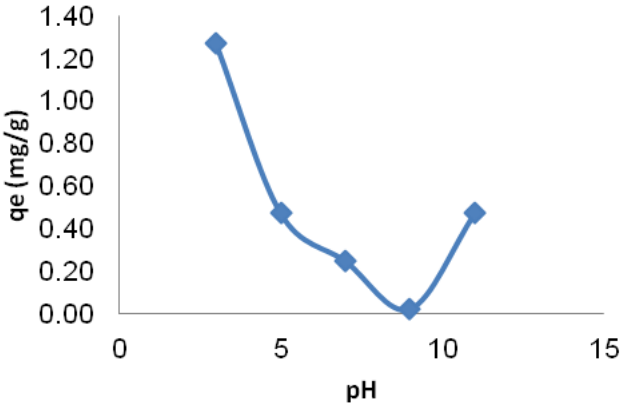

Figure 7. Effect of pH on fluoride removal by magnetic $CoFe_2O_4$NPs.

Effect of adsorbent dose: As shown in Figure 8, at pH=3 with an initial fluoride concentration of 1 mg/L, and a contact time of 60 min, increasing the dosage of adsorbent from 0.2 to 0.8 g/L reduced the amount of fluoride removal. The maximum adsorption capacity of fluoride with 0.2 g/L of adsorbent was 2.25 mg/g. Therefore, in subsequent experiments, an adsorbent dose of 0.2 g/L was selected as the optimal dose.

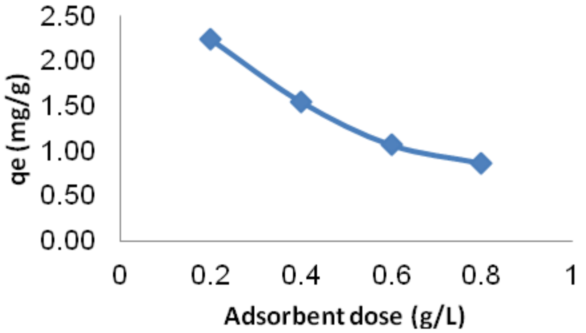

Figure 8. Effect of adsorbent dose of fluoride removal by magnetic $CoFe_2O_4$NPs.

Effect of initial fluoride concentration and contact time: Figure 9 shows the results of varying the initial fluoride concentration (1, 2, 5, and 10 mg/L) and the contact time (2, 5, 10, 20, 40, 60, and 90 min) at the optimal pH (pH=3) and adsorbent dose (0.2 g/L). The adsorption capacity, at all the concentrations of fluoride, increased with increasing contact time to 10 minutes, and then remained almost constant. The adsorption capacity with various initial fluoride concentrations (1, 2, 5, and 10 mg/L) in the first 10 minutes by the magnetic $CoFe_2O_4$NPs was 0.95, 2.55, 4.91, and 8.75 mg/g, respectively. As a result, 10 minutes was chosen as the equilibrium time.

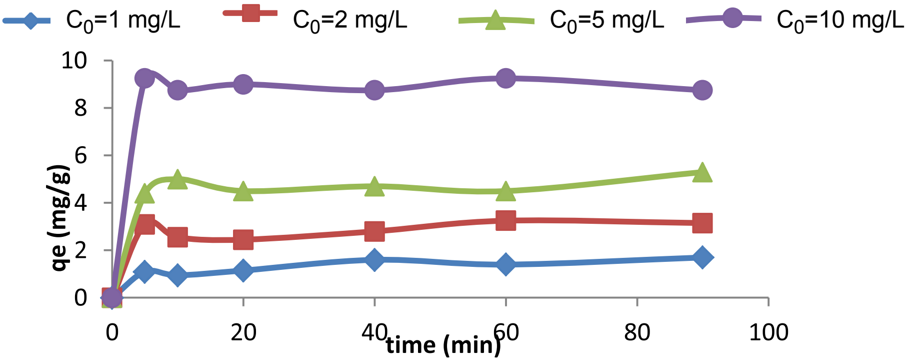

Figure 9. Effect of the initial fluoride concentration and the contact time on fluoride removal by magnetic $CoFe_2O_4$NPs.

Adsorption isotherm: The study of the absorption isotherm indicates how interactions occur between the adsorbent and the pollutant.The correlation coefficients for fluoride removal by magnetic $CoFe_2O_4$NPs with the various models are shown in Tables 1A and 1B.

Table 1A. The results of calculations for the fluoride absorption isotherms of magnetic $CoFe_2O_4$NPs for the Langmuir, Freundlichl, and BET isotherm models

Isotherm model	Constant	Value
Langmuir	q_{max} (mg/g)	14.46
	K_L (L/mg)	0.28
	R_L	0.50
	R^2	0.99
Freundlich	k_f (mg/g)	2.98
	1/n	0.68
	n	1.47
	R^2	0.96
BET	1/A.Xm	1.75
	(A-1)/(A.Xm)	1.87
	A	4.27
	Xm	2.28
	R^2	0.39

Table 1B. The results of calculations of the fluoride absorption isotherms of magnetic $CoFe_2O_4$NPs for the Temkin and Dubinin-Radushkevich isotherm models

Isotherm model	Constant	Value
Temkin	A_T, L/mg	3.31
	b_T	815.39
	B	3.04
	R^2	0.96
Dubinin-Radushkevich	β, mole²/kJ²	0.00
	E, kJ/mole	1.58
	q_m, mg/g	7.63
	R^2	0.88

The Langmuir adsorption isotherm, with a correlation coefficient R_2= 0.99, gave better results than the other isotherms.

The adherence of fluoride adsorption on magnetic $CoFe_2O_4$NPs from isotherms is as follows:

Langmuir isotherm > Freundlich isotherm > Temkin isotherm > Dubinin-Radushkevich isotherm > BET isotherm.

Adsorption kinetics: The kinetic results from the adsorption process are shown in Table 2. According to the results, the adsorption process is more correlated with second-order kinetics.

Table 2. Results of the calculations of the fluoride adsorption kinetics by magnetic $CoFe_2O_4$NPs

Adsorbent	C_0	Pseudo-first-order			Pseudo-second-order			q_e,exp(mg/g)
	(mg/L)	K_1 (min^{-1})	$q_{e,}$ cal (mg/g)	R^2	K_2 (g/mg min)	$q_{e,}$ cal(mg/g)	R^2	
$CoFe_2O_4$NPs	0.81	0.02	0.92	0.82	0.12	1.70	0.98	1.80
	1.84	0.00	1.37	0.08	0.13	3.22	0.99	4.25
	4.30	0.00	1.51	0.03	0.12	5.10	0.99	6.30
	8.00	0.00	1.14	0.14	0.53	8.85	1.00	10.25

Effect of temperature and thermodynamic parameters on fluoride adsorption by magnetic $CoFe_2O_4$NPs: Determination of the standard enthalpy and entropy parameters (ΔH and Δs) and the Gibbs free energy is important for studying the effect of temperature and the thermodynamics of fluoride adsorption. The effect of temperature on the thermodynamic parameters of the fluoride adsorption process by magnetic $CoFe_2O_4$NPs was investigated at temperatures of 288K, 298K, 308K, and 318K (Table 3 and Figure 10).

Table 3. The values of the thermodynamic parameters of fluoride adsorption under optimal conditions

Adsorbent	T (K)	qe (mg/g)	Thermodynamics Parameters		
			ΔG (kJ/mol)	ΔH (kJ/mol)	ΔS (J/mol K)
$CoFe_2O_4$NPs	288	5	0.82	23.37	78.09
	298	6.25	0.21		
	308	8.5	-0.75		
	318	9	-0.96		

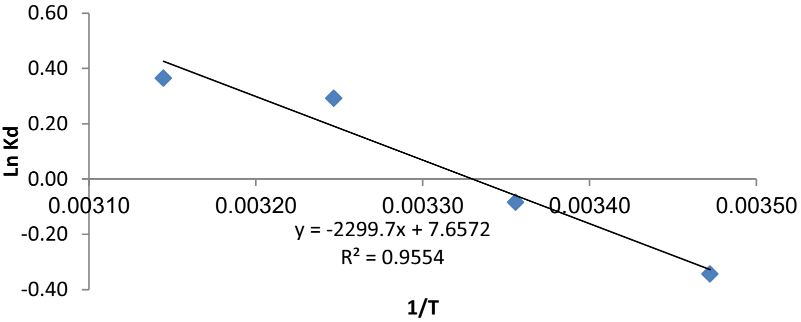

Figure 10. Effect of temperature on fluoride removal by magnetic $CoFe_2O_4$NPs.

DISCUSSION

According to the findings of this research, the pHzpc for magnetic cobalt ferrite nanoparticles is about 7.3. Investigations show that at pHs higher and lower than 3, the adsorbent surface charge is negative and positive, respectively. At a pH above 3, due to the presence of more hydroxyl anions, negative charge is induced on the absorbent surface. Therefore, at these pHs, due to the anionic nature of fluoride, an electrostatic repulsion force between the adsorbent and fluoride is produced and the amount of fluoride absorption decreases. However, at lower pHs, the number of protons increases and, when placed on the adsorbent surface, raise the adsorption power and electrostatic force between the adsorbent and fluoride which has an anionic nature.[39] Wajima et al. found that the highest removal efficiency for removing fluoride occurred at pH=3.[40]

Our results show that as the dose of adsorbent is increased the amount of fluoride adsorption per gram of adsorbent dose is reduced. The reason for this phenomenon is the non-use of all active sites at the adsorbent surface, which reduces the adsorption capacity of fluoride by magnetic $CoFe_2O_4$NPs. These results are consistent with the results of the 2016 study by Naghizadeh et al.[35]

The adsorption capacity increases with an increase in the contact time. This is due to there being more contact with the adsorbent and the increase is more in the early minutes and that, with increasing contact time, the absorption capacity reaches the equilibrium level. This can be due to a lower concentration of the fluoride solution and a reduction in the number of active sites at the adsorbent surface because, in the early stages of adsorption, a lot of vacant spaces are available on the adsorbent and these places are quickly occupied by fluoride molecules. As a result, the amount of absorption reaches equilibrium.

The initial concentration of fluoride in the adsorption process has a significant impact. The adsorption capacity increased with increasing the fluoride concentration because the increase in fluoride concentration increases the mass driving force and leads to the transfer of more molecules of fluoride on to the surface of the nanoparticles.[41] The present research is consistent with the results of a study by Asgari et al. on the removal of fluoride.[42]

Our results showed that the adsorption process follows the Langmuir adsorption isotherm. The Langmuir isotherm is based on a single layer adsorption on a homogeneous surface and there is no interaction between the adsorbed molecules.[39] For the absorption process it is desirable that $1 > R_L > 0$. These results are consistent with the study on the removal of fluoride by Sujana et al.[43]

We found the pseudo-second-order kinetics, with a correlation coefficient $R^2=1$, explained the study data better than the pseudo-first-order kinetics with $R^2=0.14$. In a pseudo-second-order kinetic model it is assumed that the adsorption process is carried out by chemical absorption, in which electron transfer occurs between the adsorbent and the adsorbate. This is consistent with the study on fluoride removal by Yuxin et al. who also found the process complied with the pseudo-second-order kinetics.[44]

The standard enthalpy and standard entropy were positive with values of 23.37 (kJ/mol) and 78.09 (J/mol), respectively. The Gibbs free energy values decreased at the temperature rose from 288K to 318K and was negative at 308K and 318K. When the ΔH is positive the fluoride adsorption process by nanoparticles is an endothermic reaction and the adsorption of this ion is more favorable at high temperatures. When the ΔS is positive the increase in temperature increases the efficiency in the common solid and liquid phases. A negative ΔG indicates that the adsorption process becomes spontaneous as the temperature rises. Our findings are consistent with those of Viswanathan, et al. on the removal of fluoride who showed that the adsorption process is spontaneous and endothermic.[45]

CONCLUSION

The SEM and TEM analyses indicate that the size of the magnetic $CoFe_2O_4NPs$ was less than 100 nm. The properties of the magnetic $CoFe_2O_4NPs$ were determined by FTIR and XRD analyses. By determining the magnetic property, we found that the strong magnetic nanoparticles formed had a magnetic saturation of 42 emu/g (ms). In this study, the optimal values of the parameters were pH=3, adsorbent dosage=0.2 g/L, initial fluoride concentration=10 mg/l, and contact time=10 min. The study of kinetics and adsorption isotherms showed that the adsorption process is more consistent with the Langmuir isotherm and the pseudo-second-order kinetics. The thermodynamics of the process showed that the values of ΔS and ΔH were positive, the ΔG value was negative at the higher temperatures of 308K and 318K, and the process was spontaneous and endothermic.

ACKNOWLEDGEMENT

We thank the Birjand University of Medical Sciences (BUMS), Iran, for their financial support of this research. The authors are also grateful to the staff of the Medical Toxicology and Drug Abuse Research Center (MTDRC) for the assisting with the analyses.

REFERENCES

1 Amini M, Mueller K, Abbaspour KC, Rosenberg T, Afyuni M, Møller KN, et al. Statistical modeling of global geogenic fluoride contamination in groundwaters. Environ Sci Technol 2008;42(10):3662-8.

2 Maheshwari R. Fluoride in drinking water and its removal. J Hazard mater 2006;137(1):456-63.

3 Sehn P. Fluoride removal with extra low energy reverse osmosis membranes: three years of large scale field experience in Finland. Desalination. 2008;223(1-3):73-84.

4 Awasti S, Gupta S, Awasti S. Sources responsible for increase in fluoride concentration in ground water and its prescribed standards. Indian J Environ Prot 2002;22(2):228.

5 Bazrafshan E, Khoshnamvand N, Mahvi AH. Fluoride removal from aqueous environments by $ZnCl_2$-treated eucalyptus leaves as a natural adsorbent. Fluoride. 2015;48(4):315-20.

6 Fan X, Parker D, Smith M. Adsorption kinetics of fluoride on low cost materials. Water Res 2003;37(20):4929-37.

7 Miretzky P, Cirelli AF. Fluoride removal from water by chitosan derivatives and composites: a review. J. Fluorine Chem 2011;132(4):231-40.

8 Mohapatra M, Anand S, Mishra BK, Giles DE, Singh P. Review of fluoride removal from drinking water. J Environ Manage 2009;91(1):67-77.

9 World Health Organization. Guidelines for drinking-water quality. 3rd ed. Vol 1. Recommendations. Geneva: World Health Organization; 2004.

10 Grandjean P. Developmental fluoride neurotoxicity: an updated review [review]. Environmental Health 2019;18:110. Available from: https://doi.org/10.1186/s12940-019-0551-x

11 Asgari G, Roshani B, Ghanizadeh G. The investigation of kinetic and isotherm of fluoride adsorption onto functionalize pumice stone. J Hazard Mater 2012;217:123-32.

12 Poureslami H, Khazaeli P, Mahvi AH, Poureslami K, Poureslami P, Haghani J, et al. Fluoride level in the breast milk in Koohbanan, a city with endemic dental fluorosis. Fluoride 2016;49(4 Pt 2):485-94.

13 Amini H, Haghighat GA, Yunesian M, Nabizadeh R, Mahvi AH, Dehghani MH, et al. Spatial and temporal variability of fluoride concentrations in groundwater resources of Larestan and

Gerash regions in Iran from 2003 to 2010. Environmental Geochemistry and Health 2016;38(1):25-37.

14 Rahmani A, Rahmani K, Dobaradaran S, Mahvi A. H, Mohamadjani R, Rahmani H. Child dental caries in relation to fluoride and some inorganic constituents in drinking water in Arsanjan, Iran. Fluoride 2010 43(3):179-86.

15 Dobaradaran S, Fazelini F, Mahvi A.H, Hosseini SS. Particulate airborne fluoride from an aluminum production plant in Arak, Iran. Fluoride 2009;42(3):228-32.

16 Mohammadi AA, Yousefi M, Yaseri M, Jalilzadeh M, Mahvi AH. Skeletal fluorosis in relation to drinking water in rural areas of West Azerbaijan, Iran. Sci Rep 2017;7(1):17300. Available from: https://doi.org/10. 1038/s41598-017-17328-8.

17 Mohammadi AA, Yousefi M, Mahvi AH. Fluoride concentration level in rural area in Poldasht city and daily fluoride intake based on drinking water consumption with temperature. Data Brief 2017;13:312–315. Available from: https://doi.org/10.1016/j.dib.2017.05.045.

18 Faraji H, Mohammadi AA, Akbari-Adergani B, Saatloo NV, Lashkarboloki G, Mahvi AH. Correlation between fluoride in drinking water and its levels in breast milk in Golestan Province, northern Iran. Iran J Public Health 2014;43(12):1664-8.

19 Yousefi M, Mohammadi AA, Yaseri M, Mahvi AH. Epidemiology of fluoride and its contribution to fertility, infertility, and abortion: an ecological study in West Azerbaijan Province, Poldasht County, Iran. Fluoride 2017;50(3):343-53.

20 Raichur A, Basu MJ. Adsorption of fluoride onto mixed rare earth oxides. Sep Purif Technol 2001;24(1-2):121-7.

21 Bazrafshan E, Ownagh KA, Mahvi AH. Application of electrocoagulation process using iron and aluminum electrodes for fluoride removal from aqueous environment. J Chem 2012;9: 2297-308.

22 Amor Z, Bariou B, Mameri N, Taky M, Nicolas S, Elmidaoui A. Fluoride removal from brackish water by electrodialysis. Desalination 2001;133(3):215-23.

23 Zazouli MA, Mahvi AH, Dobaradaran S, Barafrashtehpour M, Mahdavi Y, Balarak D. Adsorption of fluoride from aqueous solution by modified *Azolla filiculoides*. Fluoride 2014; 47(4):349-58.

24 Viswanathan N, Meenakshi S. Enhanced fluoride sorption using La (III) incorporated carboxylated chitosan beads. J Colloid Interface Sci 2008;322(2):375-83.

25 Li Y-H, Wang S, Cao A, Zhao D, Zhang X, Xu C, et al. Adsorption of fluoride from water by amorphous alumina supported on carbon nanotubes. Chem Phys Lett 2001;350(5-6):412-6.

26 Tor A. Removal of fluoride from an aqueous solution by using montmorillonite. Desalination 2006;201(1-3):267-76.

27 Nemade P, Rao AV, Alappat B. Removal of fluorides from water using low cost adsorbents. Water Sci Technol 2002;2(1):311-7.

28 Onyango MS, Kojima Y, Aoyi O, Bernardo EC, Matsuda H. Adsorption equilibrium modeling and solution chemistry dependence of fluoride removal from water by trivalent-cation-exchanged zeolite F-9. J Colloid Interface Sci 2004;279(2):341-50.

29 Hajipour AR, Khorsandi Z. A comparative study of the catalytic activity of Co-and $CoFe_2O_4$-NPs in C–N and C–O bond formation: synthesis of benzimidazoles and benzoxazoles from o-haloanilides. New J Chem 2016;40(12):10474-81.

30 Rodríguez-Rodríguez AA, Martínez-Montemayor S, Leyva-Porras CC, Longoria-Rodríguez FE, Martínez-Guerra E, Sánchez-Domínguez M. $CoFe_2O_4$-TiO_2 Hybrid Nanomaterials: Synthesis approaches based on the oil-in-water microemulsion reaction method. J Nanomater 2017;2017.Available from: http://downloads.hindawi.com/journals/jnm/2017/2367856.pdf

31 Zhao F, Zou Y, Lv X, Liang H, Jia Q, Ning W. Synthesis of $CoFe_2O_4$-zeolite materials and application to the adsorption of gallium and indium. J Chem Eng Data 2015;60(5):1338-44.

32 Saffari J, Ghanbari D, Mir N, Khandan-Barani K. Sonochemical synthesis of $CoFe_2O_4$ nanoparticles and their application in magnetic polystyrene nanocomposites. Ind Eng Chem 2014;20(6):4119-23.

33 Ben Amor T, Kassem M, Hajjaji W, Jamoussi F, Ben Amor M, Hafiane A. Study of defluoridation of water using natural clay minerals. J Clays Clay Miner 2018;66:493-99.

34 Chen H, Zhao J, Wu J, Dai G. Isotherm, thermodynamic, kinetics and adsorption mechanism studies of methyl orange by surfactant modified silkworm exuviae. J Hazard Mater 2011;192(1):246-54.

35 Bhaumik M, Leswifi TY, Maity A, Srinivasu V.V, Onyango M. Removal of fluoride from aqueous solution by polypyrrole/F_3O_4 magnetic nanocomposite. J Hazard Mater 2011;186(1):150-9.

36 Özacar M, Şengil İA. Adsorption of metal complex dyes from aqueous solutions by pine sawdust. Bioresour Technol 2005;96(7):791-5.

37 Şeker A, Shahwan T, Eroğlu AE, Yılmaz S, Demirel Z, Dalay MC. Equilibrium, thermodynamic and kinetic studies for the biosorption of aqueous lead (II), cadmium (II) and nickel (II) ions on *Spirulina platensis.* J Hazard Mater 2008;154(1-3):973-80.

38 Li XH, Xu CL, Han XH, Qiao L, Wang T, Li FS. Synthesis and magnetic properties of nearly monodisperse $CoFe_2O_4$ nanoparticles through a simple hydrothermal condition. Nanoscale Res Lett 2010;5(6):1039-44.

39 Ghaemi M, Absalan G, Sheikhian L. Adsorption characteristics of Titan yellow and Congo red on $CoFe_2O_4$ magnetic nanoparticles. J Iran Chem Soc 2014;11(6):1759-66.

40 Wajima T, Umeta Y, Narita S, Sugawara K. Adsorption behavior of fluoride ions using a titanium hydroxide-derived adsorbent. Desalination 2009;249(1):323-30.

41 Zazouli MA, Belarak D, Karimnezhad F, Khosravi F. Removal of fluoride from aqueous solution by using of adsorption onto modified *Lemna minor*: Adsorption isotherm and kinetics study. Journal of Mazandaran University of Medical Sciences 2014;23(109):195-204.

42 Asgari G, Seid Mohammadi A, Mehralipour J, Ahmadzadeh A. Performance of fluoride adsorption by snail shell in aqueous. Pajouhan Scientific Journal 2013;11(2):39-47.

43 Sujana M, Anand S. Fluoride removal studies from contaminated ground water by using bauxite. Desalination 2011;267(2-3):222-7.

44 Ma Y, Shi F, Zheng X, Ma J, Gao C. Removal of fluoride from aqueous solution using granular acid-treated bentonite (GHB): Batch and column studies. J Hazard Mater 2011;185(2-3):1073-80.

45 Viswanathan N, Sundaram CS, Meenakshi S. Removal of fluoride from aqueous solution using protonated chitosan beads. J Hazard Mater 2009;161(1):423-30.